Molecular Catalysis 593 (2026) 115765

Contents lists available at ScienceDirect

Molecular Catalysis

journal homepage: www.journals.elsevier.com/molecular-catalysis

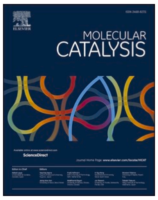

Selective hydrogenation of citral: A catalytic challenge

Stefano Paganelli [a,b,**], Chiara D'Acunzi [a], Serena Riela [c], Marina Massaro [d], Alessandro Di Michele [e], Beatrice Muzzi [f], Oreste Piccolo [g,*]

[a] Dipartimento di Scienze Molecolari e Nanosistemi, Università Ca' Foscari Venezia, Via Torino 155, 30172 Venezia Mestre, Italy
[b] Consorzio Interuniversitario Reattività Chimica e Catalisi (CIRCC), Via Celso Ulpiani 27, 70126 Bari, Italy
[c] Dipartimento di Scienze Chimiche (DSC), Università di Catania, Viale Andrea Doria 6, 95125, Catania, Italy
[d] Dipartimento di Scienze e Tecnologie Biologiche, Chimiche e Farmaceutiche (STEBICEF), Università di Palermo Viale delle Scienze, Parco d'Orleans II, Ed. 17, 90128 Palermo, Italy
[e] Dipartimento di Fisica e Geologia, Università degli Studi di Perugia, Via Pascoli, 06123 Perugia, Italy
[f] Istituto di chimica dei composti organometallici (ICCOM-CNR), Sesto Fiorentino (FI), 50019
[g] Studio di Consulenza Scientifica (SCSOP), Viale Trieste 35, 53100, Siena, Italy

ARTICLE INFO

Keywords:
Citral hydrogenation
Palladium catalyst
Rhodium catalyst
K-carrageenan
Menthol and citronellal

ABSTRACT

The hydrogenation of citral was investigated using various palladium- and rhodium-based catalytic systems. We explored both Pd and Rh nanoparticles stabilized by K-carrageenan in a biphasic water/THF system, as well as several heterogeneous catalysts with low precious metal content. In particular, the heterogenous catalysts employed were Pd/Al_2O_3 (0.3% Pd w/w), Rh/Al_2O_3 (0.18% Rh w/w), and HNTs@PDA/PdNPs (0.8% Pd w/w), obtained using a site-specific polydopamine coating on the external surface of halloysite as support. Across all experiments, palladium-based catalysts consistently demonstrated superior activity and selectivity compared to their rhodium counterparts. Notably, the catalytic systems exhibit a very different selectivity. Indeed, both Pd- and Rh-based water-soluble catalysts, as well as the heterogeneous Rh/Al_2O_3 catalytic system, favor the formation of citronellal, due to the hydrogenation of the carbon-carbon double bond conjugated to the carbonyl group. In contrast, the two heterogeneous palladium-based catalysts strongly promote the formation of menthol through the cyclization of citronellal, in some cases achieving nearly complete selectivity.

1. Introduction

Terpenes are biomolecules that plants use both as a natural defense against pests and as a means of attracting insects to aid in pollination. Many terpenes have demonstrated pharmacological effects and are also active ingredients in agriculture pesticides [1]. In addition, terpenes serve as intermediates in the synthesis of valuable products. Their hydrogenation, cyclization or isomerization leads to the production of key substances used in the flavor and fragrances industry as well as in pharmaceuticals and total synthesis [2–11]. Citral (**I**) is an acyclic monoterpenoid that is extracted as a mixture of two isomers: E-(**I**) (geranial) and Z-(**I**) (neral). It has widespread applications in the food, beverage, perfumery, and formulation science industries [12]. Citral is an α,β-unsaturated aldehyde and its hydrogenation is commonly employed as a probe reaction to evaluate catalyst selectivity. This arises from the presence of a carbonyl group and two chemically distinct C=C bonds: one conjugated with the carbonyl group and one nonconjugated. The selective hydrogenation of α,β-unsaturated compounds to the formation of the desired product without any side products is still a challenge [13–19]. In fact, depending on catalyst, citral hydrogenation can yield several products, including citronellal (**IV**), geraniol (**VI**), nerol (**VII**), and citronellol (**VIII**), as well as menthol (**III**) [11,20–28] (Scheme 1).

For instance, citronellal (**IV**) is a high added-value product used as a food flavor additive for its lemongrass-like odor [12]. It is also a key synthon in the production of menthol or hydroxydihydrocitronellal [29] as well as a mosquito repellent [30]. Moreover, by double bond isomerization or cyclization in the presence of Lewis acids, an industrially relevant product such as menthol (**III**) can be obtained [11,22,31–36]. Menthol is the worldwide most used aroma compound, responsible for the taste, smell and cooling sensation of mint. Common starting materials for menthol synthesis include *m*-cresol, citral and myrcene, as well

---

* Corresponding author.
** Corresponding author at: Dipartimento di Scienze Molecolari e Nanosistemi, Università Ca' Foscari Venezia, Via Torino 155, 30172 Venezia Mestre, Italy.
E-mail addresses: spag@unive.it (S. Paganelli), oreste.piccolo@scsop.it (O. Piccolo).

https://doi.org/10.1016/j.mcat.2026.115765
Received 8 November 2025; Received in revised form 19 January 2026; Accepted 27 January 2026

as other substrates like menthone, mono- and bicyclic terpenes, and terpenoids [32]. Many synthetic pathways rely on citronellal, cyclization of citronellal as a key step, as seen in the Takasago [37–40] and BASF processes [41–49]. Citral hydrogenation has been extensively studied using both heterogeneous and homogeneous catalysts [11, 20–28]. Supported catalysts based on metals like Pt, Ni, Ru, Rh, Pd, Au or Ir have been employed, with selectivity strongly influenced by the metal type, support material, and reaction conditions [11]. As a matter of fact, acidic or basic support materials (e.g. zeolites, natural minerals, rare earth element oxides) can promote citronellal (**IV**) conversion to isopulegol (**II**) or facilitate carbonyl acetalization in the presence of alcoholic solvents. Optimal reaction conditions can suppress these side reactions. Ni- and Pd-based catalysts without any further modification selectively produce citronellal, whereas Ni, in the second hydrogenation step, further hydrogenates the carbonyl group to yield citronellol (**VIII**). Pt catalysts exhibit low selectivity, whereas other metals favor the production of nerol and geraniol [11]. Dilute alloy catalysts have also shown high activity in citral hydrogenation, with product selectivity heavily dependent on the host metal [18]. Recently, an aqueous suspension of CTACl-capped palladium nanoparticles achieved 95% selectivity for citronellal under mild conditions (5 bar H_2, 25°C) with a metal loading of only 0.01% and a turnover number (TON) of 10,000 [21]. Besides heterogeneous catalysts, citral hydrogenation has also been carried out by using homogeneous metal complexes, which are particularly relevant for asymmetric hydrogenation and catalytic transfer hydrogenation using alternative reducing agents [11]. Furthermore, citral can be converted into various products via enzymatic or electrochemical reduction [11]. The use of supercritical CO_2 as a solvent or ionic liquids as additives or catalyst modifiers has shown promise in selectively producing citronellal, geraniol, and nerol from citral [11]. Given our interest in fine chemicals synthesis through catalytic reactions, we explored the efficiency of palladium- and rhodium-based catalysts in the selective hydrogenation of citral. Recently, our research has focused on developing water-soluble catalysts by interacting metal salts with bio-based polymers such as carboxymethyl cellulose and chitosan [50,51]. Building on this, we investigated the preparation and characterization of Pd(0) and Rh(0) nanoparticles stabilized by K-carrageenan and their catalytic performance in citral hydrogenation. K-carrageenan (Fig. 1) is a sulfonated water-soluble galactan obtained primarily from the tropical alga *Kappaphycus alvarezii*, commonly known as *Eucheuma cottonii* [52]. It is widely used in food products, pharmaceuticals, cosmetics, and oil well drilling fluids as a gelling, stabilizing, and thickening agent [53].

In catalysis, K-carrageenan can act as an efficient stabilizing agent for metal nanoparticles in aqueous media. Its negatively charged surface contains sulfate, carboxyl, hydroxyl, and ester groups that readily interact with positively charged metal ions through electrostatic attraction [52]. In this work, Pd(0) and Rh(0) nanoparticles were synthesized by mixing $Pd(NO_3)_2$ or $RhCl_3 \cdot 3H_2O$ with an aqueous K-carrageenan solution, followed by reduction with $NaBH_4$, according to established protocols [50,51,54]. The catalytic activity and selectivity of Pd(0) and Rh(0)-K-carrageenan nanoparticles were tested in water and water/organic media. We also wanted to evaluate the activity and selectivity of some heterogeneous catalysts with low precious metal content, such as Pd/Al_2O_3 (Pd 0.3% w/w) and Rh/Al_2O_3 (Rh 0.18% w/w), which were prepared using a method developed in our laboratory [55–57]. These catalysts have demonstrated high activity in hydrogenation and hydroformylation reactions [55,56,58]. Finally, we tested a newly developed Pd-based supported catalyst, prepared using a halloysite-based nanomaterial as support for metal nanoparticles [57, 59]. The support was obtained by modifying the external surface of halloysite nanotubes (HNTs) through a polydopamine (PDA) coating on ZnONPs previously anchored on the HNTs (HNTs@PDA) [60–62]. This modification, leveraging the basic properties of ZnO, enabled site-specific functionalization of the clay surface and the immobilization of Pd nanoparticles with a small and narrow size distribution. The resulting catalyst, named HNTs@PDA/PdNPs, contains 0.8% Pd (w/w) [62].

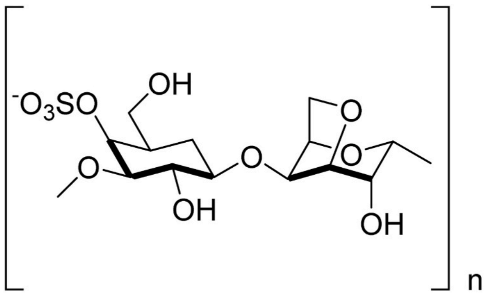

Fig. 1. K-carrageenan.

2. Experimental section

2.1. Materials and chemicals

All commercially available reagents, solvents, and chemicals were provided by Sigma Aldrich (Italy) and used as received. K-Carrageenan was a generous gift from Cargill. Alumina was generously provided by Chimet. The catalyst and products were characterized by different analytical and spectroscopic analysis such as GC, GC-MS, SEM XRD, TEM and XPS. Gas–chromatography (GC) analyses were performed on an Agilent 6850 gas chromatograph. Gas chromatography–mass spectrometry (GC–MS) analyses were performed on a HP 5890 series II gas chromatograph interfaced to a HP 5971 quadrupole mass detector. Scanning electron microscopy (SEM) was carried out using a FE-SEM LEO 1525 91 ZEISS (Jena, DE). The acceleration potential voltage was maintained at 15 keV and measurements were carried out using an In-lens detector. Samples were deposited on conductive carbon adhesive tape and metallized by sputtering with chromium (8nm). Transmission electron Microscopy (TEM) images were obtained using a TALOS F200X G2 (Thermo-Fisher Scientific) at an accelerating voltage of 200 kV using a high-speed CETA camera operating at a camera resolution of 4096 × 4096 pixels without any objective aperture. The Energy Dispersive X-ray Spectroscopy (EDS) maps were taken with a Super X spectrometer equipped with four 30 mm^2 silicon drift detectors with a collection angle of 0.7 srad. The samples were prepared by putting one drop of an

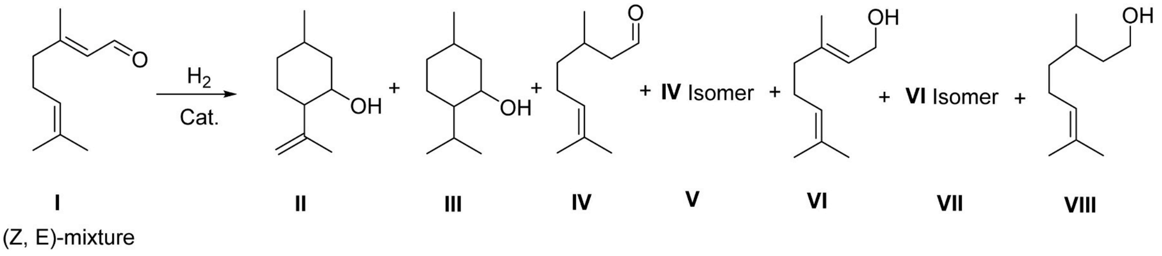

Scheme 1. Citral (**I**) hydrogenation products.

ethanol dispersion of the catalyst powder on a copper grid pre-coated with a Formvar film and dried in air.

2.2. Preparation of MNP(0)s/K-carrageenan

Preparation of Pd(0) and Rh(0) nanoparticles stabilized with K-carrageenan using $NaBH_4$ as reductant was carried out starting from $Pd(NO_3)_2x2H_2O$ or $RhCl_3x3H_2O$, respectively. The preparation of MNP(0)/K-carrageenan nanoparticles was carried out as follows: under nitrogen atmosphere, 24.3 mg (0.057 mmol) of K-carrageenan and 20 mL of distilled water, were introduced into a 100 mL flask and left under stirring until a homogeneous solution was formed. Then, 0.0143 mmol of $Pd(NO_3)_2x2H_2O$ or $RhCl_3x3H_2O$, dissolved in 1 ml of H_2O, were added to the solution and 12.5 mg (0.33 mmol) of $NaBH_4$, dissolved in 5 mL of H_2O, were added. The resulting black solution was kept under stirring for 24 h under inert atmosphere and portions of the solution used for catalytic reactions.

2.3. General procedure for the synthesis of HNTs@PDA/PdNPs nanomaterial

$PdCl_2$ (5 mg, 0.028 mmol) and NaCl (24 mg, 0.42 mmol) in water (1 mL) were heated at 80°C until $PdCl_2$ was dissolved. The obtained clear reddish solution of sodium tetrachloropalladate was cooled at room temperature and added dropwise to a suspension of HNTs@PDA (400 mg) in water (8 mL). The suspension was stirred at room temperature for 16 h, then filtered and washed several times with water to remove the unreacted materials. The solid obtained was re-suspended in ethanol (6 mL) and to the obtained dispersion a solution of $NaBH_4$ (19 mg, 0.42 mmol) in ethanol (2 mL) was added dropwise. The dispersion was stirred at room temperature for 6 h. After this time, the solvent was filtered off and the powder was washed several times with water and then dried overnight at 60°C. The amount of Pd in the nanomaterial was estimated by TGA to be as large as 0.8 wt% [62].

2.4. Preparation of Pd/Al_2O_3 (0.3% Pd w/w) and of Rh/Al_2O_3 (0.18% Rh w/w)

The catalysts were prepared by following a procedure described by some of us, by stirring $Pd(NO_3)_2x2H_2O$ or $RhCl_3x3H_2O$ and alumina in CPME, in the presence of TOA, under H_2 pressure at room temperature for 24h [55–57].

2.5. General procedure for the hydrogenation of citral (I) catalyzed by MNP(0)s/K-carrageenan

In a 50 mL test tube, equipped with a magnetic stir bar, citral (**I**), Pd- or Rh-based catalyst, water and THF were added under an inert nitrogen atmosphere. The tube was then transferred into a 150 mL stainless steel autoclave under nitrogen, pressurized with hydrogen and maintained under stirring at the desired temperature for the due time (see Tables for amounts and reaction conditions). The reactor was then cooled to room temperature, and the residual gases were released. Diethyl ether (5 ml) was added to the reaction mixture and the organic phase separated, dried on Na_2SO_4 and analyzed by GC and GC-MS. The recovered aqueous catalytic solution was used in recycling experiments.

*GC-MS m/z (**II**):* 154 (12) $[M]^+$; 139 (20) $[M\text{-}CH_3]^+$; 136 (32) $[M\text{-}H_2O]^+$; 121 (53) $[M\text{-}H_2O\text{-}CH_3]^+$; 95 $[M\text{-}H_2O\text{-}CH_2\text{-}CH_3]^+$.

*GC-MS m/z (**III**):* 156 (2) $[M]^+$; 138 (27) $[M\text{-}H_2O]^+$; 123 (31) $[M\text{-}H_2O\text{-}CH_3]^+$; 95 (70) $[M\text{-}H_2O\text{-}CH_3\text{-}CH\text{-}CH_3]^+$; 71 (100) $[CH_2CHOHCHCH_2CH_2]^+$.

*GC-MS m/z (**IV**):* 154 (10) $[M]^+$; 139 (9) $[M\text{-}CH_3]^+$; 111 (20) $[M\text{-}CH_2CHO]^+$; 95 (44) $[(CH_3)_2CCHCH_2CH_2C]^+$; 69 (99) $[(CH_3)_2CCHCH_2]^+$; 41 (100) $[CH_2CH_2CH]^+$.

*GC-MS m/z (**V**):* 154 (6) $[M]^+$; 139 (5) $[M\text{-}CH_3]^+$; 111 (18) $[M\text{-}CH_2CHO]^+;]^+$; 95 (40) $[(CH_3)_2CCHCH_2CH_2C]^+$; 69 (100) $[(CH_3)_2CCHCH_2]^+$; 41 (95) $[CH_2CH_2CH]^+$.

*GC-MS m/z (**VI**):* 154 (2) $[M]^+$; 139 (3) $[M\text{-}CH_3]^+$; 136 (15) $[M\text{-}H_2O]^+$; 121 (25) $[136\text{-}CH_3]^+$; 71 (100) $[CH_3CCHCH_2OH]^+$;41 (62) $[CH_2CH_2CH]^+$.

*GC-MS m/z (**VII**):* 154 (2) $[M]^+$; 139 (2) $[M\text{-}CH_3]^+$; 136 (10) $[M\text{-}H_2O]^+$; 121 (15) $[136\text{-}CH_3]^+$; 71 (100) $[(CH_3)_2CCHCH_2]^+$;41 (60) $[CH_2CH_2CH]^+$.

2.6. General procedure for the hydrogenation of citral (I) catalyzed by Pd- or Rh-based heterogeneous catalysts

In a 50 mL test tube, equipped with a magnetic stir bar, citral (**I**), Pd- or Rh-based catalyst and *i*-propanol were added under an inert nitrogen atmosphere. The tube was then transferred into a 150 mL stainless steel autoclave under nitrogen, pressurized with hydrogen and maintained under stirring at the desired temperature for the due time (see Tables for amounts and reaction conditions). The reactor was then cooled to room temperature, and the residual gases were released. The reaction mixture was centrifuged at 5000 rpm for 20' and the organic phase was analyzed by GC and GC-MS. The recovered solid catalyst was used in recycling experiments.

3. Results and discussion

3.1. Preparation and characterisation of MNP(0)/K-carrageenan

M(0)NPs/K-carrageenan nanoparticles were easily prepared by adding $Pd(NO_3)_2x2H_2O$ or $RhCl_3x3H_2O$ as catalyst precursor to an aqueous solution of K-carrageenan at room temperature, followed by reduction with $NaBH_4$. Pre-reduction with $NaBH_4$ was carried out following a similar procedure reported in the literature [52]. This mild synthetic approach enables the formation of metal nanoparticles stabilized by K-carrageenan. Prior to reduction, K-carrageenan interacts with the metal cations through electrostatic coordination involving sulfate ($–OSO_3^-$), hydroxyl (–OH), and ether (C–O–C) functionalities, generating a cage-like polymeric environment around the metal centers. This interaction restricts metal ion mobility and suppresses premature aggregation. Upon addition of $NaBH_4$, reduction of the metal cations occurs, leading to the formation of metallic nanoparticles embedded within the carrageenan matrix (Fig. 2). The polymer chains provide both steric and electrostatic stabilization: steric hindrance ensures spatial separation of individual nanoparticles, while negatively charged sulfate groups generate electrostatic repulsion. As a result, K-carrageenan acts as an efficient dispersing and stabilizing agent, enabling the formation of well-dispersed metal nanoparticles with controlled dimensions [63–66].

The catalysts were characterized by SEM, TEM and EDX analyses before and after catalytic use (Fig. 3).

The SEM – TEM analyses of the rhodium-based catalyst (Fig. 3a, a'), before use, highlighted that the metal particles have dimensions of about 10 nanometers for Rh(0) and a homogeneous distribution within the polymer matrix. The mapping performed on Rh(0)/K-carrageenan by EDX highlighted a homogeneous dispersion of the metal within the polymer matrix and no regions with higher metal concentrations were observed, denoting the absence of nanoparticle aggregation. After catalytic use, SEM and TEM analyses of Rh(0)/κ-carrageenan (Fig. 3b, b′) showed a slight increase in particle size compared to the fresh catalyst; however, a homogeneous dispersion within the polymer matrix was retained. EDX mapping again confirmed uniform metal distribution, with no detectable aggregation phenomena. SEM -TEM analyses of the Pd-based catalyst (Fig. 3c, c'), before use, highlighted that the metal particles have dimensions of about ten nanometers for Pd (0) and a homogeneous distribution within the polymer matrix. Mapping performed on Pd(0)/K-carrageenan by EDX highlighted a homogeneous dispersion of the metal within the polymer matrix and no regions with higher metal concentrations were observed, denoting the absence of nanoparticle aggregation. After catalytic application (Fig. 3d, d′), Pd

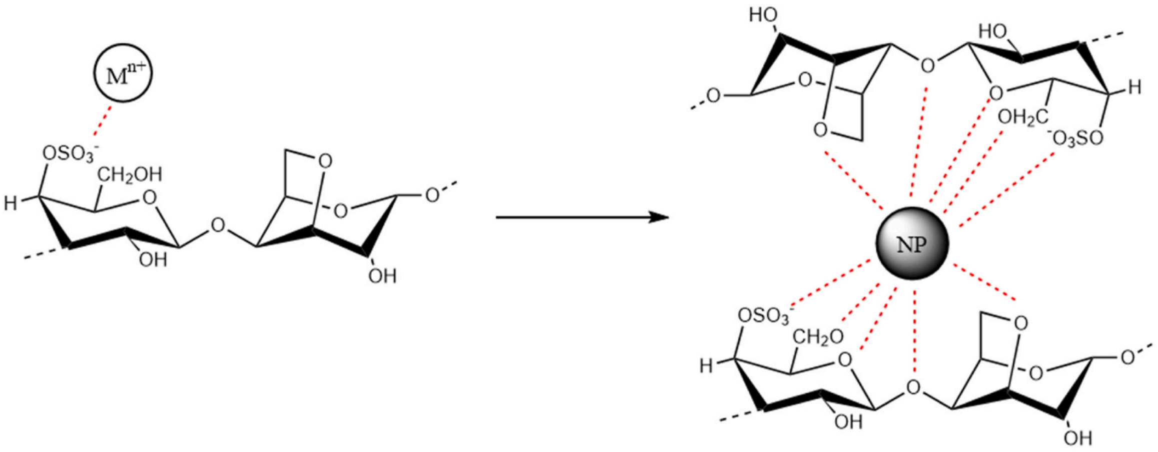

Fig. 2. Interaction between metal nanoparticles and K-carrageenan before and after the addition of $NaBH_4$.

nanoparticles exhibited a modest increase in size, analogous to the behavior observed for the rhodium system. Nevertheless, EDX mapping confirmed that palladium remained evenly distributed throughout the polymer matrix, indicating that nanoparticle aggregation was effectively prevented during catalysis.

3.2. Preparation and characterisation of HNTs@PDA/PdNPs

The HNTs@PDA/PdNPs catalyst was prepared according to procedure reported elsewhere [62], as schematized in Fig. 4. In particular, a site-specific polydopamine coating on halloysite's external surface was exploited as support for the synthesis of small and uniform in size PdNPs. The catalytic species were synthetized by a two-step procedure, involving firstly the immobilization of tetrachloropalladate ions ($PdCl_4^{2-}$) ions on the HNTs based support, followed by their *in situ* reduction by means of $NaBH_4$. Following this approach, PdNPs with a diameter of ca. 3.8 ± 0.6 nm, as estimated from statistical analysis on HR-TEM images (Figure S1), were obtained, with a percentage of Pd(0) of 78% as found by XPS measurements. The Pd3d spectrum indeed, shows the presence of two doublets at ca. 335 and 340 eV, due to typical spin-orbit splitting (Pd3d5/2 and Pd3d3/2 components) and the concomitant presence of two species of palladium, namely, Pd(0) and Pd(II) (Figure S2). TGA analysis carried out under air flow was used to perform the exact quantification of the Pd metal content that results to be as large as 0.8 wt % [62]. On the basis of the weight loss at around 800°C, it is possible to calculate the Pd loading from the O_2 evolution arising from PdO decomposition (formed under oxidizing conditions) to metallic Pd [62].

3.3. Catalytic hydrogenation of citral (I)

3.3.1. Hydrogenation of citral (I) catalyzed by MNP(0)s/K-carrageenan

The catalytic performance of Pd/K-carrageenan nanoparticles pre-reduced with $NaBH_4$ was first evaluated in the hydrogenation of citral (**I**), and the results are summarized in Table 1. All reactions were performed in a THF/H_2O mixture at 40°C, maintaining a substrate-to-palladium molar ratio of 1000:1. The first reaction, conducted at 1 MPa H_2 for 3 hours, achieved complete conversion with 89% selectivity towards citronellal (**IV**) (entry 1). Owing to the high catalytic activity, both hydrogen pressure and reaction time were reduced, resulting in complete conversion and increased selectivity toward citronellal (**IV**) (92%, entry 2), indicating that the Pd-based system efficiently discriminates between the conjugated C=C bond and other reducible functionalities under these conditions. The catalyst remained active over two recycling experiments; however, at the third recycle, conversion significantly dropped to 57%, while selectivity to citronellal (**IV**) remained high at 86% (entry 2_{r3}). Further reducing H_2 pressure to 0.1 MPa conversion lowered to 59%, but selectivity towards (**IV**) increased substantially to 95% (entry 3), consistent with suppression of consecutive hydrogenation events at reduced surface hydrogen coverage. To enhance substrate conversion, the reaction time was extended to 2 hours (run 4), raising conversion to 97%, albeit with a modest decrease in selectivity (85%, entry 4). The concomitant decrease in conversion at low pressure, and its recovery upon extending reaction time (entry 4), supports a kinetic regime in which hydrogen availability primarily controls rate, whereas selectivity is maximized when over-hydrogenation pathways are disfavored. Recyclability experiments revealed a progressive loss in activity after multiple cycles, with conversion dropping markedly in the third reuse while selectivity remained relatively high. This behavior is consistent with partial catalyst deactivation (e.g., nanoparticle growth-aggregation or poisoning), while the intrinsic chemoselectivity of the remaining active sites is largely preserved.

Further hydrogenation tests were conducted using the Rh/K-carrageenan catalytic system, with the results summarized in Table 2. The initial reaction, performed under conditions identical to those employed for the Pd-based catalyst, yielded only 24% conversion after 3 hours at 40°C with a substrate-to-rhodium molar ratio of 1000:1 (entry 1), though selectivity to citronellal (**IV**) was complete. To enhance substrate conversion, the substrate-to-rhodium molar ratio was reduced to 100:1, and the temperature increased to 60°C. Under these modified conditions, conversion rose to 63% after 4 hours, maintaining a high selectivity of 92% for (**IV**) (entry 2). Both catalytic activity and selectivity remained stable over two recycling experiments (entries 2_{r1} and 2_{r2}). Extending the reaction time to 18 hours further increased conversion to 96%, though selectivity declined to 81% (entry 3). The catalyst retained its activity in a subsequent recycling test (entry 3_{r1}). When the catalyst amount was reduced (substrate-to-rhodium molar ratio 200:1), conversion remained very high (95%), and selectivity improved to 88% (run 4). Overall, the K-carrageenan-based systems act as hydrogenation-selective platforms, favoring citronellal formation while largely suppressing cyclization chemistry, consistent with the absence of strongly acidic sites in the polymeric environment. Indeed, citral (**I**) can absorb to the nanoparticle surface through π-coordination of the conjugated C=C bond and/or via the carbonyl oxygen. The dominant formation of citronellal (**IV**) strongly suggests that the reaction proceeds primarily through 1,4-hydrogenation (C=C reduction) rather than 1,2-hydrogenation (C=O reduction) and that C=C hydrogenation rate is high and the subsequent conversion of (**IV**) (e.g., to citronellol or further hydrogenated/cyclized products) is comparatively slow under these conditions and within the K-carrageenan environment. K-Carrageenan plays a relevant role as it favors adsorption geometries leading to C=C reduction (π-binding) by attenuating strong carbonyl coordination, limits the residence time of (**IV**) at the metal surface through solvation/partitioning effects suppressing over-hydrogenation and disfavors acid-

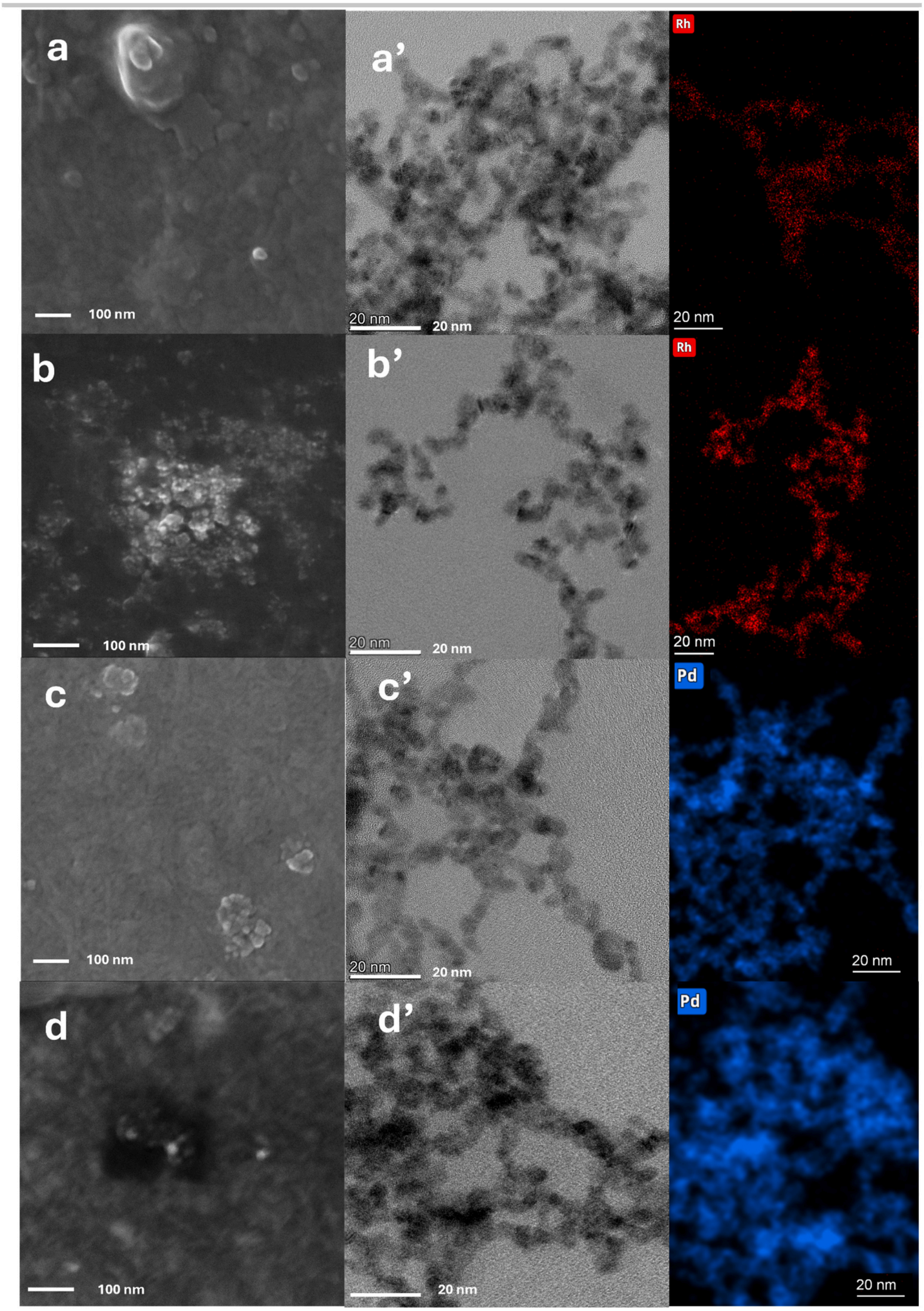

Fig. 3. SEM (a,b,c,d), TEM (a',b',c',d') images and EDX maps of Rh(0)/K-carrageenan, Rh(0)/K-carrageenan after use and Pd(0)/K-carrageenan and Pd(0)/K-carrageenan after use, respectively.

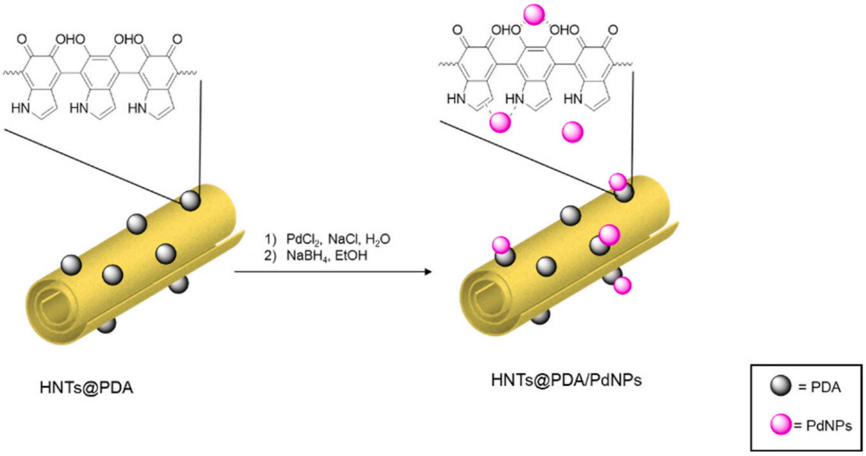

Fig. 4. Schematic representation of the synthesis of HNTs@PDA/PdNPs catalyst.

Table 1
Hydrogenation of citral (I) catalyzed by Pd/K-carrageenan.

Entry[a]	p(H_2) MPa	t(h)	Conv. (%)[b]	II yield (%)[b]	III yield (%)[b]	IV yield (%)[b]	V yield (%)[b]	TOF h^{-1}
1	1	3	100	1	4	89	6	333
2	0.2	1	100	1	3	92	4	1000
2_{r1}[c]	“	“	100	1	5	88	6	1000
2_{r2}[c]	“	“	95	1	3	86	5	950
2_{r3}[c]	“	“	57	1	3	49	4	570
3	0.1	1	59	/	1	56	2	590
4	0.1	2	97	2	6	82	7	485

[a] Reaction conditions: Substrate (I) 1.2 mmol (0.2 ml); (I)/Pd (molar ratio) = 1000; Solvent: H_2O/THF 1/1 v/v (4 mL); T = 40°C.
[b] Data determined by GC (%) using *n*-undecane as internal standard.
[c] r = recycling experiment.

Table 2
Hydrogenation of citral (I) catalyzed by Rh/K-carrageenan.

Entry[a]	S/Rh (mol)	T (°C)	t (h)	Conv. (%)[b]	II yield (%)[b]	III yield (%)[b]	IV yield (%)[b]	V yield (%)[b]	VI yield (%)[b]	VII yield (%)[b]	TOF h^{-1}
1	1000	40	3	24	/	/	24	/	/	/	80
2	100	60	4	63	/	2	58	3	/	/	16
2_{r1}[c]	“	“	“	69	/	4	54	4	3	4	17
2_{r2}[c]	“	“	“	65	/	2	56	2	2	3	16
3	100	60	18	96	/	4	78	3	5	6	5
3_{r1}[c]	“	“	“	94	/	4	76	3	6	5	5
4	200	60	18	95	/	3	84	4	4	/	1

[a] Reaction conditions: Substrate (I) 1.2 mmol (0.2 ml); Solvent: H_2O/THF 1/1 v/v (4 mL); p(H_2) = 0.2 MPa.
[b] Data determined by GC (%) using *n*-undecane as internal standard.
[c] r = recycling experiment.

catalyzed cyclization routes (citronellal → isopulegol → menthol) because K-carrageenan is not expected to provide the cooperative Lewis/Brønsted acidity and confined geometry required for efficient intramolecular cyclization.

3.3.2. Hydrogenation of citral (I) catalyzed by HNTs@PDA/PdNPs

The catalytic activity of HNTs@PDA/PdNPs was evaluated in citral hydrogenation, and the results are summarized in Table 3. All reactions were conducted at 40°C. Under mild conditions (substrate-to-Pd ratio of 1000:1, 0.2 MPa H₂, 3 h), complete conversion was achieved, with menthol (**III**) obtained as the sole product (entry 1). This selectivity markedly differs from that observed for the water-soluble Pd- and Rh-based catalysts. The different selectivity observed for the two catalytic systems can be ascribed to the heterogeneous nature of halloysite. Indeed, it possesses surfaces with different chemical compositions, providing Brønsted and Lewis acid sites that favor the cyclization of citronellal (**IV**), produced by the catalytic hydrogenation of citral to isopulegol (**II**), which is subsequently reduced to menthol (**III**). It has been hypothesized that firstly citronellal (**IV**) was formed by hydrogenation mediated by PdNPs present at the HNTs external surface,and then, diffuses into the halloysite lumen [67], where aluminol groups are located; these act as Lewis acid sites, promoting the formation of isopulegol (**II**) and, consequently, menthol (**III**). This hypothesis was further supported by the results obtained using Al_2O_3 as support (see *infra*) which does not possess an hollow tubular structure. In three recycling experiments (1_{r1}, 1_{r2}, and 1_{r3}), complete conversion was maintained; however, selectivity toward menthol (**III**) gradually decreased, with increasing amounts of isopulegol (**II**) and citronellal (**IV**) observed. Reducing the reaction time to 1 hour (entry 2), still resulted in complete conversion, though selectivity shifted: menthol (**III**) remained the primary product, but 20% of citronellal (**IV**) and trace amounts of isopulegol (**II**) were also detected. XPS analysis of the catalyst after and before use (Fig. 5, left and right side) revealed a significant decrease in Pd(0) content, from 78% to 17.5%. Despite this reduction, catalytic activity remained nearly unchanged, suggesting that palladium is reactivated by hydrogen under reaction conditions.

Table 3
Hydrogenation of citral (I) catalyzed by HNTs@PDA/PdNPs (Pd 0.8% w/w).

Entry[a]	S/Pd (mol)	$p(H_2)$ (Mpa)	t (h)	Conv. (%)[b]	II yield (%)[b]	III yield (%)[b]	IV yield (%)[b]	V yield (%)[b]	VI yield (%)[b]	VII yield (%)[b]	TOF h^{-1}
1	1000	0.2	3	99	/	99	/	/	/	/	330
1_{r1}[c]	“	“	“	>99	2	96	/	1	/	1	333
1_{r2}[c]	“	“	“	>99	1	88	11	/	/	/	333
1_{r3}[c]	“	“	“	>99	2	79	17	2	/	/	333
2	1000	0.2	1	99	2	75	20	2	/	/	990
2_{r1}[c]	“	“	“	99	3	45	47	4	/	/	990
2_{r2}[c]	“	“	“	86	2	20	52	4	6	2	860
2_{r3}[c]	“	“	“	59	1	7	30	3	16	2	590
3	1000	0.1	1	>99	1	93	5	/	/	1	1000
3_{r1}[c]	“	“	“	89	4	26	49	4	4	2	890
3_{r2}[c]	“	“	“	88	3	24	52	4	3	2	880
4	2000	0.2	3	>99	/	98	/	/	2	/	667
4_{r1}[c]	“	“	“	>99	/	98	/	/	2	/	667
5	5000	0.2	3	55	2	9	23	2	7	12	917
6	5000	0.2	16	58	2	11	20	2	9	14	181

[a] Reaction conditions: Substrate (I) 1.2 mmol (0.2 ml); Solvent: *i*-propanol (12 mL); T = 40°C.
[b] Data determined by GC (%) using *n*-undecane as internal standard.
[c] r = recycling experiment.

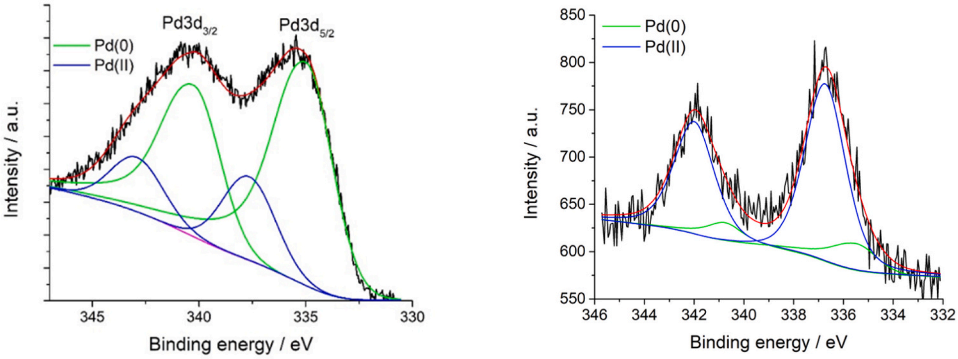

Fig. 5. XPS measurements on HNTs@PDA/PdNPs before (left side) and after (right side) use.

However, in subsequent recycling experiments (2_{r1}, 2_{r2}, and 2_{r3}), both conversion and selectivity shifted significantly, with citronellal (**IV**) replacing menthol (**III**) as the main product. Lowering the hydrogen pressure to 0.1 MPa (entry 3) resulted in complete conversion with high selectivity toward menthol (**III**) (94%). However, in the recycling experiments (3_{r1} and 3_{r2}), conversion declined, and citronellal (**IV**) became the predominant product, indicating a shift in selectivity. To explain the reduced selectivity toward menthol (**III**) observed after the recycling experiments, it was hypothesized that the diffusion of citronellal into the halloysite lumen is somehow hindered, probably due to the presence of menthol molecules from previous reactions, which can establish hydrogen-bonding interactions with aluminol groups [68]. XPS analysis of the recycled catalyst (3_{r1}) detected no Pd(0) content (Fig. 6). Nonetheless, the catalyst retained its activity, likely due to palladium reactivation by hydrogen during the reaction. Due to the high activity of the catalyst, a substrate-to-palladium molar ratio of 2000:1 was evaluated. After 3 hours at 0.2 MPa hydrogen pressure, complete conversion and high selectivity toward menthol (**III**) were achieved (entry 4), with identical results observed in a recycling test (entry 4_{r1}). However, further reducing the catalyst amount (substrate-to-Pd molar ratio of 5000:1) led to a significant decline in both conversion and selectivity (entry 5). Extending the reaction time to 16 hours under these conditions did not improve the outcome, as conversion and selectivity remained largely unchanged.

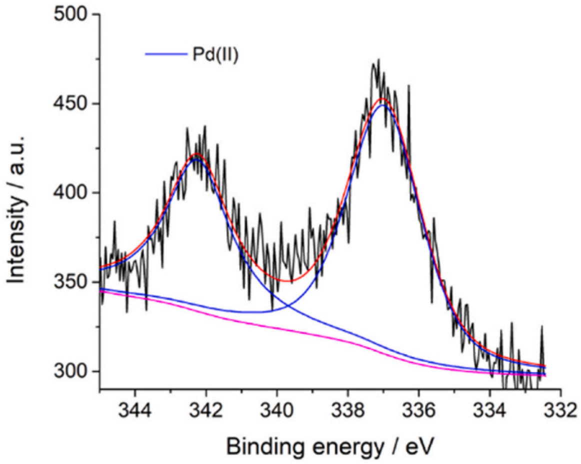

Fig. 6. XPS measurements on recycled HNTs@PDA/PdNPs (run 3_{r1} of Table 3).

3.3.3. Hydrogenation of citral (I) catalyzed by Pd/Al_2O_3 (0.3% Pd w/w)

The results of the hydrogenation of citral (**I**) catalyzed by Pd/γ-Al_2O_3 (0.3% w/w Pd) are summarized in Table 4. All experiments were conducted at 40°C and 0.2 MPa of H_2. In an initial test with a substrate-to-palladium molar ratio of 1000:1 and a reaction time of 1 hour, complete conversion was achieved with nearly complete selectivity for menthol (**III**) (entry 1). Given the catalyst's high activity, the substrate to Pd molar ratio was increased to 2000:1. After 6 hours under the same conditions, total conversion was again observed, with 98% selectivity for menthol (**III**). Five recycling experiments (2_{r1}–2_{r5}) followed, all maintaining complete conversion. While high selectivity for menthol (**III**) persisted through the first three cycles, it declined to 94% in the fourth and dropped significantly to 77% in the fifth, with approximately

Table 4
Hydrogenation of citral (I) catalyzed by Pd/γ-Al_2O_3 (Pd 0.3% w/w).

Entry[a]	S/Pd	t(h)	Conv. (%)[b]	II yield (%)[b]	III yield (%)[b]	IV yield (%)[b]	V yield (%)[b]	VI yield (%)[b]	VII yield (%)[b]	TOF h^{-1}
1	1000	1	>99	/	99	/	/	/	1	1000
2	2000	6	>99	/	98	/	/	/	2	333
$\mathbf{2_{r1}}$[c]	“	“	>99	/	98	/	/	/	2	333
$\mathbf{2_{r2}}$[c]	“	“	>99	/	98	/	/	/	2	333
$\mathbf{2_{r3}}$[c]	“	“	>99	/	97	/	/	/	3	333
$\mathbf{2_{r4}}$[c]	“	“	>99	/	94	3	/	/	3	333
$\mathbf{2_{r5}}$[c]	“	“	>99	/	77	21	/	/	2	333
3	2000	3	>99	/	98	/	/	2	/	666
$\mathbf{3_{r1}}$[c]	“	“	98	2	73	17	2	2	2	653
4	2000	1	>99	1	85	10	1	1	2	2000
$\mathbf{4_{r1}}$[c]	“	“	>99	2	83	13	1	/	1	2000
$\mathbf{4_{r2}}$[c]	“	“	>99	1	87	10	/	/	2	2000
$\mathbf{4_{r3}}$[c]	“	“	89	1	70	13	1	3	2	1780
5	5000	16	97	2	41	17	2	23	/	303

[a] Reaction conditions: Substrate (**I**) 1.2 mmol (0.2 ml); Solvent: *i*-propanol (12 mL); T = 40°C; $p(H_2) = 0.2$ MPa.

[b] Data determined by GC (%) using *n*-undecane as internal standard.

[c] r = recycling experiment.

20% citronellal (**IV**) forming. The reaction time was then reduced to 3 hours (entry 3), yielding complete conversion and maintaining high selectivity (98%) to menthol (**III**). However, even in the first recycling experiment (3_{r1}), selectivity decreased, with a notable amount (17%) of citronellal (**IV**) forming. Conversion remained high at 98%, though not total. When the reaction time was further reduced to 1 hour, the catalyst maintained high activity but showed a loss of selectivity. By the third recycling test under these conditions (entry 4_{r3}), both conversion and selectivity decreased. Finally, a substrate-to-palladium molar ratio of 5000:1 was tested, requiring a 16-hour reaction time due to the lower catalyst amount. Conversion remained high (97%) but was not complete, and selectivity was significantly reduced (entry 5). The results obtained demonstrate that alumina provides an effective environment to couple hydrogenation and cyclization steps. The gradual selectivity erosion over extended recycling (entries 2_{r1}–2_{r5}) suggests progressive loss of the cyclization/hydrogenation balance, likely due to changes in Pd dispersion, partial deactivation of acidic sites, or accumulation of strongly adsorbed species. The dependence of selectivity on reaction time (entries 2 vs 3) further indicates that product distribution is controlled by the relative rates of sequential transformations in the cascade.

3.3.4. *Hydrogenation of citral (I) catalyzed by Rh/Al_2O_3 (0.18% Rh w/w)*

At last, the hydrogenation of citral (**I**) was also examined using Rh/γ-Al_2O_3 (Rh 0.18% w/w) with a substrate-to-rhodium molar ratio of 1000:1, at 40°C and 0.2 MPa hydrogen pressure, varying reaction times. The results are summarized in Table 5. After 1 hour, the reaction achieved a low conversion of 41% with nearly 90% selectivity toward citronellal (**IV**) (entry 1). A recycling test was conducted to assess potential catalyst activation, but no improvement was observed, as conversion and selectivity remained unchanged (entry 1_{r1}). Extending the reaction to 3 hours did not significantly enhance activity or selectivity (entry 2), and activity declined notably from the third recycle (entry 2_{r3}). In the final test (entry 3), increasing the reaction time to 5 hours improved conversion to 90%, though it remained incomplete. This suggests gradual catalyst activation over prolonged reaction periods. In the first recycle under these conditions (entry 3_{r1}), conversion remained stable, but a decline was observed in the second recycle (entry 3_{r2}). At all tested reaction conditions, selectivity was consistently directed toward citronellal (**IV**), but it was relatively low, reaching a maximum of only about 80%. The modest conversion increase with longer times suggests gradual activation, yet the inability to achieve high menthol selectivity indicates that, under the investigated conditions, Rh sites do not effectively promote the hydrogenation steps required to drive the cascade to completion or do not synergize as efficiently with the support acidity as Pd does.

The catalytic data (Tables 1–5) highlight the decisive roles of metal identity, support acidity/architecture, and reaction parameters in controlling both activity and product distribution in citral (**I**) hydrogenation. Two distinct reactivity regimes were observed: (i) selective hydrogenation to citronellal (**IV**) with the water-soluble K-carrageenan systems and (ii) one-pot conversion to menthol (**III**) with Pd-based heterogeneous catalysts supported on halloysite or alumina. Water-soluble Pd- and Rh-based catalysts preferentially afforded citronellal, whereas Pd-based heterogeneous catalysts—namely HNTs@PDA/PdNPs and Pd/Al_2O_3—promoted the selective formation of menthol. Rh-based catalysts consistently exhibited lower activity than their palladium counterparts. According to the literature [11,69], three types of selectivity govern citral hydrogenation: (i) differentiation between concurrent hydrogenation and cyclization reactions, (ii) competition among different reactive sites (conjugated C=C, C=O, and isolated C=C bonds), and (iii) consecutive hydrogenation of intermediate products

Table 5
Hydrogenation of citral (I) catalyzed by Rh/γ-Al_2O_3 (Rh 0.18% w/w).

Entry[a]	t (h)	Conv. (%)[b]	II yield (%)[b]	III yield (%)[b]	IV yield (%)[b]	V yield (%)[b]	VI yield (%)[b]	VII yield (%)[b]	TOF h^{-1}
1	1	41	/	2	36	/	3	/	410
$\mathbf{1_{r1}}$	“	41	/	2	35	1	3	/	410
2	3	62	/	4	53	1	4	/	207
$\mathbf{2_{r1}}$[c]	“	72	/	/	68	/	4	/	240
$\mathbf{2_{r2}}$[c]	“	85	/	13	70	2	/	/	283
$\mathbf{2_{r3}}$[c]	“	49	/	3	37	/	8	/	163
3	5	90	/	10	72	2	4	/	180
$\mathbf{3_{r1}}$	“	90	/	7	68	2	4	7	180
$\mathbf{3_{r2}}$[c]	“	69	/	4	58	2	4	/	138

[a] Reaction conditions: Substrate (**I**) 1.2 mmol (2.2 ml); (**I**)/Pd (molar ratio) = 1000; Solvent: *i*-propanol (12 mL); T = 40°C; $p(H_2) = 0.2$ MPa.

[b] Data determined by GC (%) using *n*-undecane as internal standard.

[c] r = recycling experiment.

such as citronellal. Support surface properties strongly influence these processes, while metal electronic density affects substrate adsorption and residence time [70]. Palladium catalysts typically favor citronellal formation [11,21], whereas the acidic nature of halloysite and alumina supports promotes citronellal cyclization to isopulegol and subsequent hydrogenation to menthol. The most significant finding is the high menthol selectivity achieved with Pd-based heterogeneous catalysts, particularly Pd/γ-Al_2O_3. Direct one-pot conversion of citral to menthol is industrially attractive because conventional Pd catalysts typically stop at citronellal and require a separate Lewis acid-catalyzed cyclization step followed by further hydrogenation. In the present systems, the combination of highly active Pd nanoparticles and acidic supports enables this otherwise challenging cascade within a single catalytic material, providing a practical route to menthol under mild conditions. Basing on the reported results, we can assume that the Pd/γ-Al_2O_3 catalyst likely operates via a bifunctional pathway in which Pd nanoparticles dissociate H_2 and promote the rapid 1,4-hydrogenation of citral to citronellal, whereas Lewis/weak Brønsted acidic sites on γ-Al_2O_3 facilitate the intramolecular cyclization of citronellal to isopulegol. Subsequent hydrogenation of the isopulegol C=C bond on Pd affords menthol. The progressive loss of menthol selectivity upon recycling, while maintaining full conversion, is consistent with selective deactivation of the acid function (e.g., fouling by strongly adsorbed oxygenates/oligomeric deposits), which shifts the network toward accumulation of citronellal. In contrast, Rh/γ-Al_2O_3 predominantly catalyzes the initial C=C hydrogenation step, giving citronellal as the major product; the limited formation of menthol suggests an inefficient tandem sequence, potentially due to weaker cooperation between Rh sites and the support-mediated cyclization step, as well as a slower catalyst conditioning/activation under H_2.

4. Novelty and research perspectives

Synthesis of citronellal (**IV**)

Pd nanoparticles in water, including CTACl-stabilized Pd colloids that deliver very high citronellal selectivity under mild conditions with high TON values, have been described [11,21,71]. These systems, however, often rely on surfactant-stabilized colloids and often require careful control of additives and medium acidity/basicity to suppress over-hydrogenation and other byproducts.

In this context, the Pd(0)/K-carrageenan catalyst provides two practical advantages:

1) Bio-derived stabilizer and aqueous compatibility. K-Carrageenan plays a dual role as a stabilizing matrix and dispersing agent in water-containing media, enabling high citronellal (**IV**) selectivity without the need for conventional surfactants. This aligns well with greener strategies and simplifies catalyst handling relative to many colloidal systems.
2) Tunable selectivity through mild parameter changes. The observed increase in citronellal (**IV**) selectivity at lower H_2 pressure, while maintaining substantial activity, is consistent with selectively suppressing consecutive hydrogenation pathways through reduced surface hydrogen coverage, an operational lever of clear industrial relevance.

The Rh(0)/K-carrageenan system is less active than Pd under comparable conditions but it shows excellent citronellal (**IV**) selectivity at partial conversion and good stability upon recycling once a higher catalyst loading/temperature is adopted.

Synthesis of menthol (**III**)

One-pot menthol (**III**) synthesis from citral (**I**) has been demonstrated using bifunctional catalysts, typically involving Ni or Ru metals combined with acidic supports (zeolites, aluminosilicates, clays) or heteropoly acids, often requiring higher severity (temperature and/or longer times) [11] than the mild conditions used by us. The main competitive advantages of the present Pd-based heterogeneous catalysts are:

1) Mild operating conditions with very high menthol selectivity. Achieving near-quantitative menthol selectivity at 40°C and low H_2 pressure (0.2 MPa) is notably mild compared with many reported one-pot systems that use higher temperatures, higher pressures, or continuous reactors to sustain productivity [11,33,72–79].
2) Low precious metal loadings. Pd/Al_2O_3 contains only 0.3 wt % Pd, and HNTs@PDA/PdNPs contains 0.8 wt % Pd, which is favorable relative to numerous reported bifunctional catalysts using higher metal loadings [11].
3) No external acid co-catalyst required. The menthol pathway is enabled by the intrinsic acidity of the support (alumina or halloysite), avoiding addition of homogeneous Lewis acids or strongly acidic heteropoly acids. This simplifies process design and reduces the risk of corrosion or neutralization steps often associated with homogeneous acid catalysis.
4) One-pot cascade enabled by support architecture. The halloysite system is particularly interesting because the tubular morphology can spatially couple hydrogenation, on Pd sites, with cyclization inside/near acidic domains (e.g., aluminol groups in the lumen), conceptually resembling a “nanoreactor” that promotes the cascade.

These results open several clear development directions:

- Stability and recyclability control. The selectivity drift observed upon recycling, especially for HNTs@PDA/PdNPs, suggests that long-term performance depends on preserving Pd surface state and dispersion, and accessibility/strength of acidic sites responsible for cyclization. Future work should target mitigation of pore/lumen blocking (e.g., by product adsorption) and maintaining the metal–acid balance.
- Support acidity and architecture tuning. Since cyclization is rate- and selectivity-determining in the cascade reaction, tuning of acidity (type and strength of Lewis/Brønsted sites) and transport properties (mesoporosity, lumen accessibility) could improve robustness. Comparative studies on non-tubular acidic supports versus halloysite could clarify whether confinement effects are a decisive factor.
- Lower metal content and higher productivity. The strong activity at substrate/Pd up to 2000 suggests the feasibility of further reducing Pd usage by optimizing dispersion and metal–support interfacial chemistry. Also, the use of bimetallic Pd–(Ni, Cu, Ru) catalysts could promote the reaction at higher substrate/metal ratios, while keeping mild conditions.
- Process translation to flow and scale-up. The mild batch conditions here employed provide a strong foundation for developing a continuous flow system, particularly if catalyst stability and mass-transfer limitations can be addressed.
- Expanding sustainable catalyst platforms. Other bio-derived, water-soluble polymers (polysaccharides, lignin derivatives, modified celluloses) may enable tunable hydrogenation selectivity in aqueous media, thus using a wide range of sustainable catalysts.

5. Conclusion

New water-soluble MNPs(0)/K-carrageenan nanoparticles were readily prepared by mixing ($Pd(NO_3)_2{\cdot}2H_2O$ or $RhCl_3{\cdot}3H_2O$) with K-carrageenan in an aqueous solution, followed by reduction with $NaBH_4$. These catalytic systems were characterized before and after use via SEM, TEM, and EDX analyses, which confirmed a homogeneous dispersion of the nanoparticles within the polymer matrix and the absence of nanoparticle aggregation. Additionally, a new heterogeneous Pd-based catalyst, HNTs@PDA/PdNPs, was prepared using as support a site-specific polydopamine coating on the external surface of halloysite. HR-TEM analysis revealed PdNPs with a diameter of approximately 3.8 ± 0.6 nm, while XPS measurements indicated that 78% of the Pd was in the Pd(0) oxidation state. TGA analysis performed under airflow allowed for precise quantification of the Pd metal content, which was determined to be 0.8 wt%. Beside these catalytic species, low-metal-content catalysts such as Pd/Al_2O_3 (0.3% Pd w/w) and Rh/Al_2O_3 (0.18% Rh w/w) were synthesized by stirring $PdCl_2·2H_2O$ or $RhCl_3·3H_2O$ with alumina in CPME, in the presence of trioctyl amine (TOA), under H_2 pressure at room temperature for 24 hours, following a procedure previously reported by some of us [55–57]. All catalytic systems were tested in the hydrogenation of citral, an acyclic monoterpenoid widely used in the food, beverage, perfumery, and formulation industries [12]. The selective hydrogenation of citral is challenging due to the potential formation of numerous products, including citronellal, geraniol, nerol, citronellol, dihydrocitronellal [11,20–28], and menthol, the most widely used aroma compound worldwide [11,22,31–36]. Menthol formation can occur through double-bond isomerization or cyclization in the presence of Lewis acids. All tested catalytic systems exhibited excellent activity and recyclability, achieving complete conversions. However, selectivity was highly catalyst-dependent. Specifically, water-soluble catalytic species favored the formation of citronellal, whereas Pd-based heterogeneous catalysts, i.e. HNTs@PDA/PdNPs and Pd/Al_2O_3, predominantly produced menthol, a result of considerable industrial relevance The best catalytic performance was observed with Pd/Al_2O_3 (0.3% Pd w/w). At a substrate-to-Pd molar ratio of 2000:1, this catalyst achieved total conversion at 40°C and 0.2 MPa H_2 after just 6 hours, with near-complete selectivity toward menthol. Remarkably, both its activity and selectivity remained practically unchanged over five recycling experiments. While extending the reaction time to 16 hours at a higher substrate-to-Pd molar ratio of 5000:1 resulted in 97% conversion, selectivity significantly decreased. All tested rhodium catalysts exhibited lower activity. Some results obtained in this research are highly promising, particularly with a view to potential future industrial applications. Indeed, the present work offers a selectivity-divergent platform: K-carrageenan-stabilized Pd or Rh catalysts favor citronellal (**IV**) under mild conditions, whereas Pd on acidic heterogeneous supports enables direct menthol (**III**) formation from citral (**I**) in a single pot, at low temperature and low hydrogen pressure. We are currently conducting further studies to explore other commercially available water-soluble bio-derived materials for metal nanoparticle anchoring, novel MNPs(0)/halloysite catalytic systems, and low-metal-content bimetallic catalysts. These investigations aim to evaluate and compare their performances in hydrogenation reactions with those of the catalytic species reported in this work.

CRediT authorship contribution statement

Stefano Paganelli: Writing – review & editing, Writing – original draft, Methodology, Conceptualization. **Chiara D'Acunzi:** Investigation, Formal analysis. **Serena Riela:** Writing – original draft, Methodology, Formal analysis, Conceptualization. **Marina Massaro:** Methodology, Investigation, Formal analysis. **Alessandro Di Michele:** Methodology, Investigation, Formal analysis. **Beatrice Muzzi:** Investigation, Data curation. **Oreste Piccolo:** Writing – review & editing, Writing – original draft, Methodology, Investigation, Conceptualization.

Declaration of competing interest

The authors declare that they have no known competing financial interests or personal relationships that could have appeared to influence the work reported in this paper.

Acknowledgements

The authors express their gratitude to Cargill for generously supplying K-carrageenan and to Chimet for providing alumina. XPS analyses were performed at the ATeN Center–University.

Supplementary materials

Supplementary material associated with this article can be found, in the online version, at doi:10.1016/j.mcat.2026.115765.

Data availability

Data will be made available on request.

References

[1] H.S. Stoker, General, Organic and Biological Chemistry, 4th edition, Houghton Mifflin Company, Boston, 2007, p. 337.

[2] F. Lefebvre, J-P. Candy, C.C. Santini, J-M. Basset, Surface organometallic chemistry on metals. Application to chemicals and fine chemicals, Top. Catal. 4 (1997) 211.

[3] W.F. Hoelderich, Environmentally benign manufacturing of fine and intermediate chemicals, Catal. Today 62 (2000) 115.

[4] P. Kraft, J.A. Bajgrowicz, C. Denis, G. Fráter, Odds and trends: recent developments in the chemistry of odorants, Angew. Chem. Int. Ed. 39 (2000) 2980.

[5] C. Chapuis, J. Jacoby, Catalysis in the preparation of fragrances and flavours, Appl. Catal. A Gen. 221 (2001) 93.

[6] K.A.D. Swift, Catalytic Transformations of the Major Terpene Feedstocks, Top. Catal. 27 (2004) 143.

[7] N. Ravasio, F. Zaccheria, M. Guidotti, R. Psaro, Mono and Bifunctional Heterogeneous Catalytic Transformation of Terpens and Terpenoids, Top. Catal. 27 (2004) 157.

[8] J.L.F. Monteiro, C.O. Veloso, Catalytic Conversion of Terpenes into Fine Chemicals, Top. Catal. 27 (2004) 169.

[9] B. Chen, U. Dingerdissen, J.G.E. Krauter, H.G.J.L. Rotgerink, K. Möbus, D. J. Ostgard, P. Panster, T.H. Piermeier, S. Seebald, T. Tacke, H. Trauthwein, New developments in hydrogenation catalysis particularly in synthesis of fine and intermediate chemicals, Appl. Catal. A Gen. 280 (2005) 17.

[10] A. Corma, M. Renz, M. Susarte, Transformation of Biomass Products into Fine Chemicals Catalyzed by Solid Lewis and Brønsted-acids, Top. Catal 52 (2009) 1182.

[11] A. Stolle, T. Gallert, C. Schmöger, B. Ondruschka, Hydrogenation of citral: a wide-spread model reaction for selective reduction of α,β-unsaturated aldehydes, RSC. Adv. 3 (2013) 2112.

[12] J.B Sharmeen, F.M. Mahomoodally, G. Zengin, F. Maggi, Essential oils as natural sources of fragrance compounds for cosmetics and cosmeceuticals, Molecules. 26 (2021) 666.

[13] V. Ponec, On the role of promoters in hydrogenations on metals; α,β-unsaturated aldehydes and ketones, Appl. Catal., A 149 (1997) 27.

[14] P. Claus, Selective hydrogenation of a,β-unsaturated aldehydes and other C=O and C=C bonds containing compounds, Top. Catal. 5 (1998) 51.

[15] P. Mäki-Arvela, J. Hájek, T. Salmi, D.Y. Murzin, Chemoselective hydrogenation of carbonyl compounds over heterogeneous catalysts, Appl. Catal. A Gen. 292 (2005) 1.

[16] H. Ye, H. Zhao, Y. Jiang, H. Liu, Z. Hou, Catalytic transfer hydrogenation of the C=O bond in unsaturated aldehydes over Pt nanoparticles embedded in porous UiO-66 nanoparticles, ACS Appl. Nano Mat. 3 (2020) 12260.

[17] M. Yu, H. Ma, X. Ma, W. Zhao, Q. Zhu, J. Li (Shandong NHU Pharmaceutical Co. Ltd.; Zhejiang NHU Co. Ltd.), CN114939438A, 2022.

[18] D. Wu, J. Zhang (Southeast University), CN112536038A, 2021.

[19] L. Yu, W. Fang, H. Zhu, K. Li, Y. Zhang, Y. Shen, J. Dong (Wanhua Chemical Group Co. Ltd.), CN112121794A, 2020.

[20] E. Bailón-García, F.J. Maldonado-Hódar, A.F. Pérez-Cadenas, F. Carrasco-Marín, Catalysts supported on carbon materials for the selective hydrogenation of citral, Catalysts. 3 (2013) 853.

[21] M. Duval, G. Sagorin, A. Denicourt-Nowicki, A. Roucoux, Highly selective and multigram hydrogenation of citral into citronellal by palladium nanoparticles in water, ACS Sust. Chem. Eng. 10 (2022) 5500.

[22] M.R. Ball, L. Proaño, I. Nezam, D-C. Lee, F. Alamgir, C.W. Jones, Citral hydrogenation over dilute alloy catalysts, ChemCatChem. 15 (2023) 202201396.

[23] R.X. Liu, Y. Yu, K. Yoshida, G. Li, H. Jiang, M. Zhang, F. Zhao, S. Fujita, M. Arai, Physically and chemically mixed TiO_2-supported Pd and Au catalysts: unexpected synergistic effects on selective hydrogenation of citral in supercritical CO_2, J. Catal. 269 (2010) 191.

[24] X.-Y. Quek, Y. Guan, R.A. van Santen, E.J.M. Hensen, Ionic-liquid stabilized rhodium nanoparticles for cutral cyclodehydrogenation, ChemSusChem. 3 (2010) 1264.

[25] T. Ekou, L. Ekou, A. Vicente, G. Lafaye, S. Pronier, C. Especel, P.J. Marécot, Citral hydrogenation over Rh and Pt catalysts supported on TiO_2: influence of the preparation and activation protocols of the catalysts, J. Mol. Catal. A Chem 337 (2011) 82.

[26] J. Holz, S. Doerfelt, A. Börner, Manufacture of Citronellal by the Rhodium-Catalyzed Homogeneous Hydrogenation of Neral, Adv. Synth. Catal. 359 (2017) 4379.

[27] U.K Singh, M.N. Sysak, M.A. Vannice, Liquid-phase hydrogenation of citral over Pt/SiO_2 catalysts: II. Hydrogenation of reaction intermediate compounds, J. Catal. 191 (2000) 181.

[28] L. Wang, N. Cao, Y. Sun, J. Dong, B. Yu (Wanhua Chemical Group Co. Ltd.), CN112121793A, 2020.

[29] E.J. Lenardao, G.V. Botteselle, F. de Azambuja, G. Perin, R.G. Jacob, Citronellal as key compound in organic synthesis, Tetrahedron. 63 (2007) 6671.

[30] E.J. Du, T.J. Ahn, M.S. Choi, I. Kwon, H.-K. Kim, J.Y. Kwon, K. Kang, The mosquito repellent citronellal directly potentiates *Drosophila* TRPA1, facilitating feeding suppression", Mol. Cells 38 (2015) 911.

[31] A. Corma, S. Iborra, A. Velty, Chemical routes for the transformation of biomass into chemicals, Chem. Rev. 107 (2007) 2411.

[32] D. Dylong, P.J.C. Hausoul, R. Palkovits, M. Eisenacher, Synthesis of (−)-menthol: Industrial synthesis routes and recent development, Flav. Fragr J 37 (2022) 195.

[33] P. Maki-Arvela, I. Simakova, Z. Vajglova, D.Y. Murzin, One-pot synthesis of menthol from citral and citronellal over heterogeneous catalysts, Catal. Surv. Asia 27 (2023) 2.

[34] F. Zaccheria, R. Psaro, N. Ravasio, Outstanding results in hydrogenation reactions over heterogeneous copper catalysts, Recent Res. Devel. Catal. 2 (2003) 23.

[35] I.L. Simakova, Z. Vajglova, M. Martinez-Klimov, K. Eranen, M. Peurla, P. Maki-Arvela, D.Y. Murzin, One-pot synthesis of menthol from citral over Ni/H-β-38 extrudates containing bentonite clay binder in batch and continuous reactors, Org. Proc. Res. Devel. 27 (2023) 295.

[36] I.M.J. Vilella, S.R. de Miguel, C. Salinas-Martinez de Lecea, A. Linares-Solano, Scelza O.A, Catalytic performance in citral hydrogenation and characterization of PtSn catalysts supported on activated carbon felt and powder, Appl. Catal. A: Gen. 281 (2005) 247.

[37] M. Emura, H. Matsuda, A green and sustainable approach: celebrating the 30th anniversary of the asymmetric L-menthol process, Chem. Biodivers. 11 (2014) 1688.

[38] S. Akutagawa, Asymmetric synthesis by metal BINAP catalysts, Appl Catal A Gen 128 (1995) 171.

[39] S. Akutagawa, Enantioselective isomerization of allylamine to enamine: practical asymmetric synthesis of (–)-menthol by Rh–BINAP catalysts, Top. Catal. 4 (1997) 271.

[40] R. Noyori, Asymmetric catalysis: science and opportunities, Adv. Synth. Catal. 345 (2003) 15.

[41] G. Wegner, G. Kaibel, J. Therre, W. Aquila, H. Fuchs (BASF AG) WO2008037693A1, 2008.

[42] W.F. Hoelderich, Environmentally benign manufacturing of fine and intermediate chemicals, Catal. Today 62 (2000) 115.

[43] D.J. Ager, J.G. de Vries, in: E.M. Carreira, H. Yamamoto (Eds.), Comprehensive Chirality, Comprehensive Chirality, 9, Elsevier Science, Amsterdam, 2012, pp. 73–82.

[44] C. Jäkel, R. Paciello, in: H.-U. Blaser, H.-J. Federsel (Eds.), Asymmetric Catalysis on Industrial Scale: Challenges, Approaches, and Solutions, Wiley-VCH, Weinheim, 2010, pp. 187–205.

[45] M. Friedrich, K. Ebel, N. Goetz, W. Krause, C. Zahm (BASF AG) WO2006092433A1, 2006.

[46] M. Friedrich, K. Ebel, N. Goetz (BASF SE), US7550633B2, 2009.

[47] G. Heydrich, G. Gralla, M. Rauls, J. Schmidt-Leithoff, K. Ebel, W. Krause, S. Oehlenschlaeger, C. Jaekel, M. Friedrich, E.J. Bergner, N. Kashani-Shirazi, R. Paciello (BASF SE) WO2009068444A2, 2009.

[48] G. Gralla, G. Heydrich, E.J. Bergner, K. Ebel, (BASF SE) WO2009013192 A1, 2009.

[49] E.J. Bergner, K. Ebel, T. Johann, O. Lober, O. Loeber, (BASF SE) US 7709688B2, 2010.

[50] S. Paganelli, E. Brugnera, A. Di Michele, M. Facchin, V. Beghetto, Chitosan as biobased ligand for the production of hydrogenation catalysts, Molecules. 29 (2024) 2083.

[51] S. Paganelli, N. Massimi, L. Cattazzo, A. Di Michele, O. Piccolo, M. Facchin, V. Beghetto, Use of carboxymethyl cellulose as binder for the production of water-soluble catalysts, Int. J. Bio. Macromol 270 (2024) 132541.

[52] E.M. Roy, E.P. Carter, G.J. Flick Jr, L.M. Davis (Eds.), B. Rudolph in *Marine and Freshwater Products Handbook*, Technomic Publishing Co, Lancaster, 2000, pp. 515–529.

[53] F. van de Velde, S.H. Knutsen, A.I. Usov, H.S. Rollema, A.S. Cerezo, 1H and 13C high resolution NMR spectroscopy of carrageenans: application in research and industry, Food Sci. Technol. 13 (2002) 73.

[54] M.A. Harrad, P. Valerga, M.C. Puerta, I. Houssini, M.A. Ali, L. El Firdoussi, A. Karim, Ni(0)-CMC-Na Nickel colloids in sodium carboxymethyl-cellulose: catalytic evaluation in hydrogenation reactions, Molecules. 16 (2011) 367.

[55] S. Paganelli, A. Angi, N. Pajer, O. Piccolo, "A smart heterogeneous catalyst for efficient, chemo- and stereoselective hydrogenation of 3-hexyn-1-ol" *Catalysts* 2021, 11, 14.

[56] O. Piccolo, I. Arčon, G. Das, G. Aquilanti, A. Prai, S. Paganelli, M. Facchin, V. Beghetto, Synthesis of Helional by hydrodechlorination reaction in the presence of mono and bi-metallic catalysts supported on alumina, Catalysts. 14 (2024) 255.

[57] M. Massaro, C.G. Colletti, G. Lazzara, S. Milioto, R. Noto, S. Riela, Halloysite nanotubes as support for metal-based catalysts, J. Mater. Chem. A 5 (2017) 13276.

[58] S. Paganelli, R. Tassini, V.D. Rathod, B. Onida, S. Fiorilli, O. Piccolo, A low rhodium content smart catalyst for hydrogenation and hydroformylation reactions, Catal. Lett. 151 (2021) 1508.

[59] M. Massaro, C.G. Colletti, G. Buscemi, S. Cataldo, S. Guernelli, G. Lazzara, L. F. Liotta, F. Parisi, A. Pettignano, S. Riela, Palladium nanoparticles immobilized on halloysite nanotubes covered by a multilayer network for catalytic applications, New J. Chem. 42 (2018) 13938.

[60] M. Massaro, M. Casiello, L. D'Accolti, G. Lazzara, A. Nacci, G. Nicotra, R. Noto, A. Pettignano, C. Spinella, S. Riela, One-pot synthesis of ZnO nanoparticles supported on halloysite nanotubes for catalytic applications, Appl. Clay Sci. 189 (2020) 105527.

[61] M.L. Alfieri, M. Massaro, M. d'Ischia, G. D'Errico, N. Gallucci, M. Gruttadauria, M. Licciardi, L.F. Liotta, G. Nicotra, G. Sfuncia, S. Riela, Site-specific halloysite functionalization by polydopamine: a new synthetic route for potential near infrared-activated delivery system, J. Col. Interface Sci. 606 (2022) 1779.

[62] M. Massaro, C. D'Acunzi, S. Paganelli, M.L. Alfieri, L.F. Liotta, A. Lopez-Galindo, R. de Melo Barbosa, O. Piccolo, R. Sánchez-Espejo, C. Viseras, S. Riela, Halloysite@ polydopamine nanoplatform for ultrasmall Pd and Cu nanoparticles: suitable catalysts for hydrogenation and reduction reactions, Catalysts. 15 (2025) 1029.

[63] J.P.O. Bantang, U.G Bigol, D.H. Camacho, Gel and Film composites of silver nanoparticles in κ-, ι-, and λ-carrageenans: one-pot synthesis, characterization, and bioactivities, Bionanoscience 11 (2021) 53.

[64] F. VandeVelde, N.D. Lourenço, H.M. Pinheiro, M. Bakker, Carrageenan: a food-grade and biocompatible support for immobilisation techniques, Adv. Synth. Catal. 344 (2002) 815.

[65] S. Leviev, A. Wolfson, O. Levy-Ontman, Novel iota carrageenan-based $RhCl_3$ as an efficient and recyclable catalyst in Suzuki cross coupling, Mol Catal 486 (2020) 110841.

[66] S. Wang, T. Vincent, C. Faur, E. Guibal, A comparison of palladium sorption using polyethylenimine impregnated alginate-based and carrageenan-based algal beads, Appl Sci 8 (2018) 264.

[67] M. Massaro, C.G. Colletti, B. Fiore, V. La Parola, G. Lazzara, S. Guernelli, N. Zaccheroni, S. Riela, Gold nanoparticles stabilized by modified halloysite nanotubes for catalytic applications, Appl. Organomet. Chem. 33 (2019) e4665.

[68] M. Massaro, S. Riela, G. Cavallaro, C.G. Colletti, S. Milioto, R. Noto, G. Lazzara, Ecocompatible Halloysite/Cucurbit[8]uril hybrid as efficient nanosponge for pollutants removal, ChemistrySelect. 1 (2016) 1773.

[69] R.L. Augustine, Catal. Today 37 (1997) 419.

[70] Y.S. Demidova, E.V. Suslov, O.A. Simakova, I.L. Simakova, K.P. Volcho, N. F. Salakhutdinov, D.Yu. Murzin, Selective carvone hydrogenation to dihydrocarvone over titania supported gold catalyst, Catal. Today 241 (2015) 189.

[71] Hongfei Huo, Lina Liang, Xinyang Zhai, Hongwei Wang, Wangxin Kong, Dewei Zhai, Dong Liu, Pengbo Jiang, Chunliang Li, Lukuan Zong, Changyan Cao, Weiguo Song, Amine-functionalized hydrophobic cross linked polymer supported palladium nanoparticles: an efficient catalyst for the selective hydrogenation of citral to citronellal, Ind. Eng. Chem. Res. 63 (2024) 6279.

[72] I. Simakova, P. Maki-Arvela, M. Martinez-Klimov, J. Muller, Z. Vajglova, M. Peurl, K. Eränen, Dmitry Yu, Murzin "Continuous synthesis of menthol from citronellal and citral over Ni-beta-zeolite-sepiolite composite catalyst, Appl. Catal. A Gen. 636 (2022) 118586.

[73] I. Simakova, P. Maki-Arvela, M. Martinez-Klimov, J. Muller, Z. Vajglova, M. Peurl, K. Eränen, Dmitry Yu, Murzin "one-pot synthesis of menthol starting from citral over Ni supported on attapulgite-H-beta-38 extrudates in a continuous flow: effect of metal location, Ind. Eng. Chem. Res. 61 (2022) 13.

[74] A.K. Shah, G. Maitlo, A.A. Shah, I.A Channa, G.A. Kandhro, H.A. Maitlo, U. H. Bhatti, A. Shah, A.Q. Memon, A.S. Jatoi, Y.H. Park, One pot menthol synthesis via hydrogenations of citral and citronellal over montmorillonite-supported Pd/ Ni-heteropoly acid bifunctional catalysts, Reaction Kinetics Mech. Catal. (2019), https://doi.org/10.1007/s11144-019-01679-6.

[75] Irina. Simakova, Z. Vajglová, M. Martínez-Klimov, K. Eränen, M. Peurl, P. Mäki-Arvela, D. Yu.Murzin, One-pot synthesis of menthol from citral over Ni/H-β-38 extrudates containing bentonite clay binderin batch and continuous reactors, Org. Proc. Res. Dev. 27 (2023) 295.

[76] S. Taghavi, E. Ghedini, F. Menegazzo, M. Signoretto, One-pot transformation of citronellal to menthol over H-beta zeolite supported ni catalyst: effect of catalyst support acidity and ni loading, Catal. Let. 153 (2023) 2674.

[77] E. Dhiaul Iftitah, M. Muchalal, W. Trisunaryanti, R. Armunanto, R. Psaro, N. Ravasio F. Santoro, L. Sordelli, One pot transformation of citronellal to menthol over Ni/γ-Al_2O_3, J. Appl. Sci. Res. 7 (2011) 680.

[78] C. Barrales Cortés, V. Tamayo Galván, S. Santiago Pedro, T.Viveros García, One pot synthesis of menthol from (±)-citronellal on nickel sulfated zirconia catalysts, Catal. Today 172 (2011) 21.

[79] J. Plößer, M. Lucas, P. Claus, Highly selective menthol synthesis by one-pot transformation of citronellal using Ru/H-BEA catalysts, J. Catal. 320 (2014) 189.